

Low-Temperature Al₂O₃ Atomic Layer Deposition

M. D. Groner,[†] F. H. Fabreguette,[†] J. W. Elam,[†] and S. M. George^{*,†,‡}

Department of Chemistry and Biochemistry and Department of Chemical Engineering,
University of Colorado, Boulder, Colorado 80309-0215

Received July 3, 2003. Revised Manuscript Received December 5, 2003

Al₂O₃ films were deposited by atomic layer deposition (ALD) at temperatures as low as 33 °C in a viscous-flow reactor using alternating exposures of Al(CH₃)₃ (trimethylaluminum [TMA]) and H₂O. Low-temperature Al₂O₃ ALD films have the potential to coat thermally fragile substrates such as organic, polymeric, or biological materials. The properties of low-temperature Al₂O₃ ALD films were investigated versus growth temperature by depositing films on Si(100) substrates and quartz crystal microbalance (QCM) sensors. Al₂O₃ film thicknesses, growth rates, densities, and optical properties were determined using surface profilometry, atomic force microscopy (AFM), QCM, and spectroscopic ellipsometry. Al₂O₃ film densities were lower at lower deposition temperatures. Al₂O₃ ALD film densities were 3.0 g/cm³ at 177 °C and 2.5 g/cm³ at 33 °C. AFM images showed that Al₂O₃ ALD films grown at low temperatures were very smooth with a root-mean-squared (RMS) roughness of only 4 ± 1 Å. Current–voltage and capacitance–voltage measurements showed good electrical properties of the low-temperature Al₂O₃ ALD films. Elemental analysis of the films using forward recoil spectrometry revealed hydrogen concentrations that increased with decreasing growth temperature. No other elements were observed by Rutherford backscattering spectrometry except the parent aluminum and oxygen concentrations. Low-temperature Al₂O₃ ALD at 58 °C was demonstrated for the first time on a poly(ethylene terephthalate) (PET) polymeric substrate. Al₂O₃ ALD coatings on PET bottles resulted in reduced CO₂ gas permeabilities.

1. Introduction

The coating of thermally fragile substrates by atomic layer deposition (ALD) may provide exciting new applications of ALD in diverse areas ranging from food packaging to microelectronics to biomaterials. For example, thin ALD films may serve as gas diffusion barriers in food packaging and extend shelf life by decreasing oxygen diffusion through potato chip bags or slowing the escape of CO₂ from pressurized soda containers.^{1,2} ALD coatings on polymers may also be important as gas diffusion barriers for flexible electronic devices or organic light emitting diodes (OLEDs).^{3,4} However, few ALD processes have been demonstrated at low temperatures of <100 °C. Room-temperature catalytic SiO₂ ALD has been demonstrated with SiCl₄ and H₂O plus pyridine⁵ or NH₃⁶ as the catalyst. ALD of ZnSe and CdS has also been demonstrated at room

temperature.⁷ The vast majority of ALD processes occur at temperatures of >100 °C that would degrade organic, polymeric, or biological material.

Al₂O₃ is one of the most widely studied materials grown by ALD.^{8–17} Al₂O₃ is a well-behaved ALD system that can be accomplished with a variety of precursors and relatively short cycle times. The effect of growth temperature on the properties of Al₂O₃ ALD films has been studied at temperatures ranging from 125 to 500 °C.^{11–16} For microelectronics applications, desired properties such as high dielectric constant and low impurity concentration have been found to be optimized at a growth temperature of ~350 °C.¹¹ Little is known about Al₂O₃ ALD at low temperatures (≤100 °C) and the

* To whom correspondence should be addressed. Phone: 303-492-3398. Fax: 303-492-5894. E-mail: steven.george@colorado.edu.

[†] Department of Chemistry and Biochemistry.

[‡] Department of Chemical Engineering.

(1) Benmalek, M.; Dunlop, H. M. *Surf. Coat. Technol.* **1995**, 77, 821.
(2) Erlat, A. G.; Spontak, R. J.; Clarke, R. P.; Robinson, T. C.; Haaland, P. D.; Tropsha, Y.; Harvey, N. G.; Vogler, E. A. *J. Phys. Chem. B* **1999**, 103, 6047.

(3) Burrows, P. E.; Bulovic, V.; Forrest, S. R.; Sapochak, L. S.; McCarty, D. M.; Thompson, M. E. *Appl. Phys. Lett.* **1994**, 65, 2922.

(4) Weaver, M. S.; Michalski, L. A.; Rajan, K.; Rothman, M. A.; Silvernail, J. A.; Brown, J. J.; Burrows, P. E.; Graff, G. L.; Gross, M. E.; Martin, P. M.; Hall, M.; Mast, E.; Bonham, C.; Bennett, W.; Zumhoff, M. *Appl. Phys. Lett.* **2002**, 81, 2929.

(5) Klaus, J. W.; Sneh, O.; George, S. M. *Science* **1997**, 278, 1934.

(6) Klaus, J. W.; George, S. M. *Surf. Sci.* **2000**, 447, 81.

(7) Luo, Y.; Slater, D.; Han, M.; Moryl, J.; Osgood, R. M. *Appl. Phys. Lett.* **1997**, 71, 3799.

(8) Ritala, M.; Leskela, M. In *Handbook of Thin Film Materials*, Vol. 1; Nawa, H. S., Ed.; Academic Press: San Diego, CA, 2001.

(9) Ott, A. W.; Klaus, J. W.; Johnson, J. M.; George, S. M. *Thin Solid Films* **1997**, 292, 135.

(10) Dillon, A. C.; Ott, A. W.; Way, J. D.; George, S. M. *Surf. Sci.* **1995**, 322, 230.

(11) Groner, M. D.; Elam, J. W.; Fabreguette, F. H.; George, S. M. *Thin Solid Films* **2002**, 413, 186.

(12) Yun, S. J.; Lee, K.; Skarp, J.; Kim, H.; Nam, K. *J. Vac. Sci. Technol. A* **1997**, 15, 2993.

(13) Matero, R.; Rahtu, A.; Ritala, M.; Leskela, M.; Sajavaara, T. *Thin Solid Films* **2000**, 368, 1.

(14) Kukli, K.; Ritala, M.; Leskela, M.; Jokinen, J. *J. Vac. Sci. Technol. A* **1997**, 15, 2214.

(15) Fan, J.; Sugioaka, K.; Toyoda, K. *Jpn. J. Appl. Phys.* **1991**, 30, L1139.

(16) Drozd, V. E.; Baraban, A. P.; Nikiforova, I. O. *Appl. Surf. Sci.* **1994**, 82/83, 583.

(17) Elam, J. W.; Groner, M. D.; George, S. M. *Rev. Sci. Instrum.* **2002**, 73, 2981.

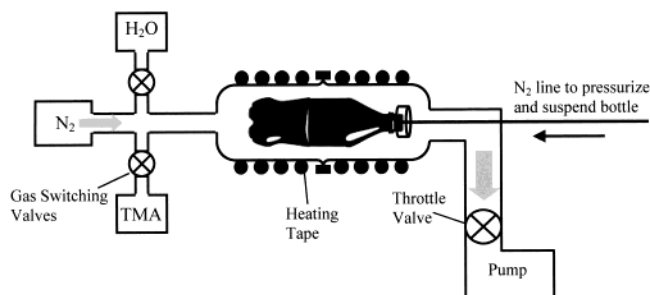


Figure 1. Diagram of the viscous-flow reactor used for low-temperature Al_2O_3 ALD. A special flow tube was employed to accommodate a 510-mL PET bottle. A nitrogen purge line was used to suspend and pressurize the PET bottle during Al_2O_3 ALD.

properties of such films. This study explores the conditions necessary for low-temperature Al_2O_3 ALD and examines the properties of the resulting films. Low-temperature Al_2O_3 ALD was also applied for the first time to a poly(ethylene terephthalate) (PET) polymer substrate. Reduced gas permeabilities were observed for Al_2O_3 ALD-coated PET bottles.

2. Experimental Section

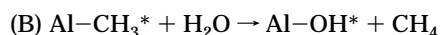
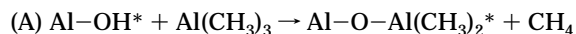
A. Chemicals and Substrates. Al_2O_3 ALD films were grown using H_2O (Fisher, optima grade) and $\text{Al}(\text{CH}_3)_3$ [trimethylaluminum (TMA)] (Akzo-Nobel, semiconductor grade, 99.9999%). The carrier gas in the viscous flow reactor was N_2 (Airgas, ultrahigh purity). Moderately doped n -type Si(100) wafers from Montco Silicon Technologies, Inc., with a boron doping density of $\sim 2 \times 10^{17} \text{ cm}^{-3}$ were used as substrates.

A variety of chemicals were used for etching and cleaning of the Si substrates. These chemicals included 5% HF (general chemicals class 10 water/HF (10:1) mix), water (HPLC grade), sulfuric acid, and hydrogen peroxide (30%). Prior to deposition, the silicon wafers were cut into $\sim 2.5 \text{ cm} \times 2.5 \text{ cm}$ pieces, cleaned in a $\sim 60^\circ\text{C}$ Piranha solution for 15 min, and then HF etched for 60 s.

For gas diffusion tests, uncoated poly(ethylene terephthalate) (PET) bottles were supplied by Applied Films Corp. The bottles were 510-mL Coke Contour bottles. These PET bottles had a weight of 28 g and a petaloid shaped base. The PET bottles were cleaned with Micro cleaner/oxide remover (International Products Corp.) prior to deposition.

B. Al_2O_3 ALD Film Growth in Viscous-Flow Reactor. Al_2O_3 films were grown by ALD in a viscous-flow ALD reactor. This reactor has been described in detail in other publications.^{11,17} TMA and H_2O were alternately entrained in the N_2 carrier flow using gas switching valves.¹⁷ The N_2 carrier gas pressure was ~ 1.0 Torr. TMA and H_2O pressure transient increases of ~ 0.1 Torr were measured by a Baratron when the reactants were introduced into the N_2 carrier flow.

The Al_2O_3 ALD film growth proceeded according to two self-limiting surface reactions. The TMA and H_2O yield Al_2O_3 ALD according to the following two reactions:^{9,10}



where the asterisks denote the surface species. When performed in an ABAB... reaction sequence, these sequential reactions produce linear, atomic-layer controlled Al_2O_3 growth. Many previous studies have confirmed linear and conformal growth using TMA and H_2O .^{9,11,15,17}

The standard flow tube was used to deposit Al_2O_3 ALD films on Si substrates or the QCM.¹⁷ Figure 1 shows the reactor with a larger-than-normal flow tube designed to accommodate the PET bottles. Figure 1 also shows a simplified diagram of the

gas switching valves and the gas reservoirs. The gas switching valves allow for a rapid turn-on and shut-off of the reactant gases for short ALD cycle times. This short time is facilitated by pumping the gas reservoirs with separate mechanical pumps after the reactant exposures.¹⁷

The time for one complete Al_2O_3 ALD cycle ranged from 12 s at 177°C to 203 s at 33°C . This cycle time was defined by (t_1, t_2, t_3, t_4) where t_1 is the TMA exposure time, t_2 is the N_2 purge time following the TMA reactant exposure, t_3 is the H_2O exposure time, and t_4 is the N_2 purge time following the H_2O reactant exposure. All times are in units of seconds. Longer purge times were required at lower temperatures to avoid Al_2O_3 chemical vapor deposition (CVD) resulting from insufficient purge times.

Quartz crystal microbalance (QCM) studies of Al_2O_3 ALD were performed in situ using a Maxtek TM400 thin-film deposition monitor. The QCM crystal housing was sealed and purged to prevent deposition on the backside and positioned horizontally in the flow reactor tube. A detailed description of the QCM for monitoring ALD has been presented in a previous publication.¹⁷

Al_2O_3 ALD films were deposited on PET bottles at 58°C . To accommodate the 510-mL PET bottles, the standard reactor flow tube was replaced with a larger 10-cm diameter tube as shown in Figure 1. This tube consisted of the bottom halves of two vacuum traps joined by an O-ring and a clamp. The bottles were suspended in this enlarged reactor tube by a custom-made cap and purge line that allowed the bottle to be pressurized with N_2 gas during Al_2O_3 ALD. The pressurization prevented bottle deformation during and after the Al_2O_3 ALD film growth.

C. Al_2O_3 Film Characterization. Al_2O_3 film thicknesses and refractive indices were measured using a J. A. Woollam M44 variable-angle spectroscopic ellipsometer (VASE). Measurements were obtained over the spectral range from 406 to 806 nm using an incidence angle of 75° . Al_2O_3 and SiO_2 have virtually identical optical constants. Consequently, a simple ellipsometric measurement yields only the sum of the Al_2O_3 and SiO_2 film thicknesses. To determine the true Al_2O_3 thickness and the thickness of any interfacial SiO_2 layer on Si(100), a procedure was employed that utilized simultaneous Al_2O_3 ALD growth on both an HF-etched Si wafer and a Si wafer with a native oxide. This procedure was described in detail in another publication.¹¹ A $13 \pm 2 \text{ \AA}$ thick interfacial SiO_2 layer was determined to be present at the Al_2O_3 /Si interface after Al_2O_3 ALD. This SiO_2 thickness was subtracted from the ellipsometric measurements to determine the Al_2O_3 layer thickness.

Atomic force microscope (AFM) images of the Al_2O_3 films and substrates were obtained using an AutoProbe CP Research scanning probe microscope (SPM) instrument from Thermo-Microscopes. RMS surface roughness values were calculated on the basis of $1 \mu\text{m}^2$ contact-mode AFM scans. Profilometry was performed using a Dektak 3 surface profile measuring system from Veeco Metrology Group. Al_2O_3 film thicknesses were determined by measuring step heights using profilometry and contact-mode AFM. Well-defined steps needed for AFM imaging were created by masking part of the sample with a small piece of high-temperature aluminum foil tape (3M, Type 433) during Al_2O_3 ALD. Other methods, such as clamping another piece of silicon to the substrate, were found to produce poorly defined steps that were too wide to be imaged by AFM.

Electrical measurements were performed using a MDC 811 mercury probe from the Materials Development Corporation. These electrical measurements have been described in another publication.¹¹ The mercury probe makes contact to the front surface of the Al_2O_3 films by drawing up a well-defined column of Hg with a surface area of 0.437 mm^2 . Current-voltage (IV) measurements were obtained using a Keithley 487 picoammeter/voltage source. Capacitance-voltage (CV) measurements were performed using a Stanford Research Systems SR720 LCR meter. The experiments were computer-controlled using LabView from National Instruments.

Elemental analysis was performed at the Ion Beam Analysis Laboratory in the Institute of Technology Characterization

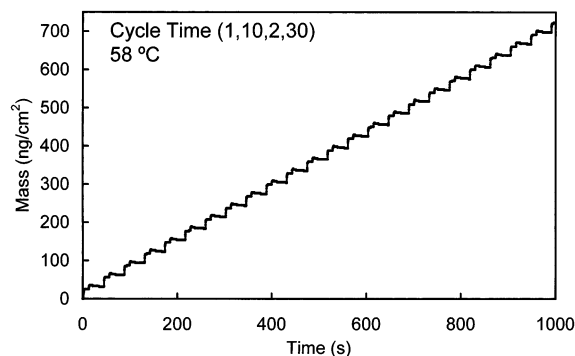


Figure 2. QCM measurements for Al₂O₃ ALD at 58 °C showing the linear growth of the Al₂O₃ ALD film over many reaction cycles. The average Al₂O₃ mass gain per ALD cycle is 30 ng/cm².

Facility at the University of Minnesota. Al and O were determined by Rutherford backscattering spectrometry (RBS) using a 3.5 MeV ⁴He²⁺ and 2.4 MeV ⁴He⁺ beam, respectively. H was determined by 1.3 MeV ⁴He⁺ forward recoil spectrometry (FReS). The instrument is composed of a NEC 1.7 MV Pelletron accelerator with a Charles Evans RBS 400 endstation. The He beam incident angle was 75°. The RBS detector was located at 165° and the FReS detector was located at 30° from the beam direction. A 5-μm-thick Mylar foil was placed in front of the FReS detector to filter the scattered ⁴He particles. The error was estimated at less than 5%.

X-ray reflectivity (XRR) was performed with a Bede Scientific Ltd. D1 System using a channel cut crystal. The X-ray wavelength from the Cu Kα X-ray tube was 1.54 Å. The electron beam current in the X-ray tube was 20 mA at 35 kV. A θ -2 θ scan was performed with a 10-arcsec step size and a 5-s acquisition time. The Bede Refs software with a genetic algorithm was used to fit the XRR data and calculate the densities of the films.

Gas diffusion tests on the Al₂O₃ ALD-coated PET bottles were performed by Applied Films Corporation using a GMS barrier measurement system (Balzers Process Systems, GmbH). The bottles were pressurized with up to 6 bar of CO₂ gas. The loss of CO₂ was then measured over 3 to 4 days. The CO₂ loss rate of an Al₂O₃ ALD-coated PET coated bottle was compared with the CO₂ loss rate of an uncoated bottle. This ratio of these loss rates determined the CO₂ barrier improvement factor (BIF).

3. Results

A. Quartz Crystal Microbalance. Al₂O₃ ALD was characterized at different growth temperatures from 33 to 177 °C using a QCM. Figure 2 shows Al₂O₃ ALD at 58 °C using a (1, 10, 2, 30) cycle time. The Al₂O₃ ALD film growth is very linear with number of ALD reaction cycles. A mass gain per cycle of 30 ng/cm² was measured for the Al₂O₃ ALD growth shown in Figure 2. A more detailed view of the QCM data is shown in Figure 3. The QCM data for three ALD cycles shows the mass gain for each TMA and water exposure. The time periods during which the TMA and H₂O dosing valves were open are denoted by the shaded regions. A larger mass gain is observed during the TMA exposure than during the H₂O exposure. This behavior is similar to that previously observed during QCM studies of Al₂O₃ ALD at 177 °C.¹⁷

The QCM data were used to determine the optimal reactant exposures and nitrogen purge times for Al₂O₃ ALD at low temperatures. At 177 °C, QCM data from this work and a previous study¹⁷ showed that 1-s exposure times and 5-s purge times were sufficient for

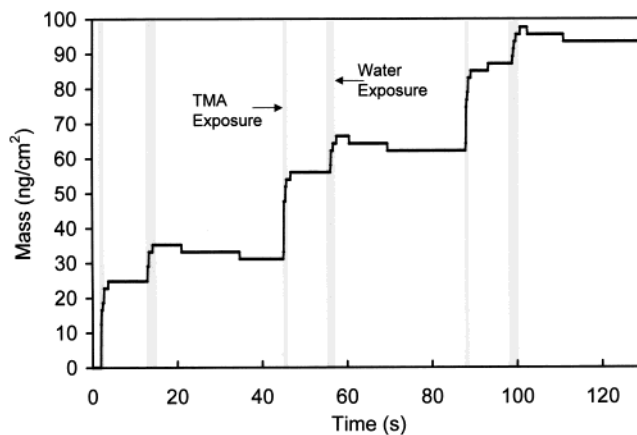


Figure 3. Detailed view of the QCM measurements at 58 °C. The shaded areas show the time periods during which the TMA and water dosing valves were open. The mass increases coincide with the TMA and water exposures.

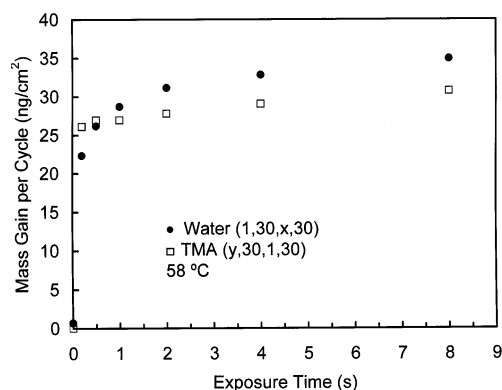


Figure 4. Al₂O₃ mass gain per cycle versus reactant exposure time at 58 °C. Purge times for both TMA and water were 30 s each. The exposure time of the reactant not being investigated was held constant at 1 s.

complete reaction and purging of all of the reactants to prevent CVD. Both the required exposure times and purge times increased with decreasing temperatures.

The dependence of the Al₂O₃ ALD mass gain on reactant exposure time at 58 °C is shown in Figure 4. These curves were obtained by monitoring QCM data while varying the individual reactant exposure times to determine the minimum precursor exposures necessary for the TMA and H₂O reactions to reach completion. Figure 5 shows the effect of purge times on the Al₂O₃ ALD growth rates. Purge times were chosen to be long enough to avoid reactant mixing and subsequent CVD. The CVD growth is indicated by the rise in mass gain per cycle at short purge times. On the basis of these studies, the optimal cycle time for Al₂O₃ ALD growth at 58 °C was (1, 10, 2, 30) where all times are in units of seconds.

QCM experiments confirmed that Al₂O₃ ALD is possible at temperatures as low as 33 °C. This temperature was the lowest temperature that could be achieved without actively cooling the viscous flow reactor. However, the required H₂O purge time was 180 s at 33 °C. Table 1 shows the reactant exposure and purge times used to perform Al₂O₃ ALD at growth temperatures ranging from 33 to 177 °C. The resulting Al₂O₃ ALD mass gains per cycle determined by the QCM are also given in Table 1.

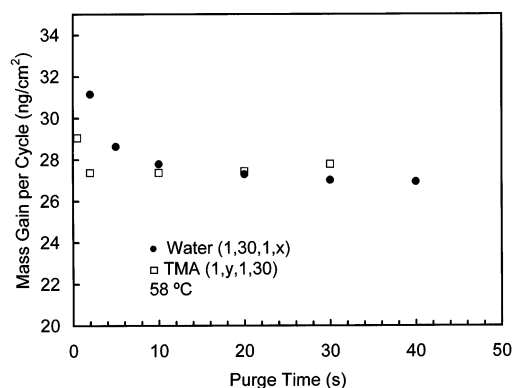


Figure 5. Al_2O_3 mass gain per cycle versus purge time at 58 °C. Exposure times for both TMA and water were 1 s each. The purge time of the reactant not being investigated was held constant at 30 s.

Table 1. Reactant Exposure Times, Purge Times, and Mass Gain Per Cycle Determined by the QCM for Al_2O_3 ALD Films Grown at Temperatures from 33 to 177 °C

	growth temperature (°C)					
	177	125	102	80	58	33
TMA exposure time (s)	1	1	1	1	1	1
purge time (s)	5	5	5	5	10	20
water exposure time (s)	1	2	2	2	2	2
purge time (s)	5	10	20	20	30	180
mass gain/cycle (ng/cm ²)	38	39	36	34	30	28

QCM measurements indicated a maximum mass gain per cycle of 39 ng/cm² at 125 °C. A slight decrease to 38 ng/cm² in the mass gain per cycle was measured at 177 °C. Below 125 °C, the mass gain per cycle decreases with decreasing growth temperature and reaches a value of 30 ng/cm² at 33 °C.

B. Spectroscopic Ellipsometry. Al_2O_3 ALD film thicknesses and the refractive index, n , were determined at wavelengths from 406 to 806 nm using spectroscopic ellipsometry. For Al_2O_3 films grown using 300 reaction cycles, the film thickness increased from 332 Å at 33 °C to 401 Å at 125 °C. The film thickness then decreased slightly to 375 Å at 177 °C. These measurements yield Al_2O_3 ALD growth rates of 1.11, 1.34, and 1.25 Å/cycle, respectively. Al_2O_3 ALD growth rates over the entire growth temperature range are given in Figure 6.

The refractive indices decreased slightly with decreasing growth temperature. The results of these measurements are also shown in Figure 6. The refractive indices varied by <1% over the spectral range from 406 to 806 nm. Consequently, the analysis was performed by assuming that the refractive index was constant over the entire wavelength range. The maximum refractive index was $n = 1.60$ at 177 °C. The refractive index decreased to $n = 1.51$ at 33 °C. Figure 6 also shows the density of the Al_2O_3 ALD films calculated on the basis of the QCM mass measurements and the ellipsometric Al_2O_3 film thicknesses.

C. Profilometry, Atomic Force Microscopy, and X-ray Reflectivity. Profilometry and AFM were used as independent measures of Al_2O_3 ALD film thicknesses. Figure 7 shows a $10 \times 10 \mu\text{m}^2$ AFM image used to determine the thickness of an Al_2O_3 ALD film grown at 58 °C using 300 reaction cycles on a Si(100) substrate. The step was created by covering part of the sample with high-temperature aluminum tape during Al_2O_3

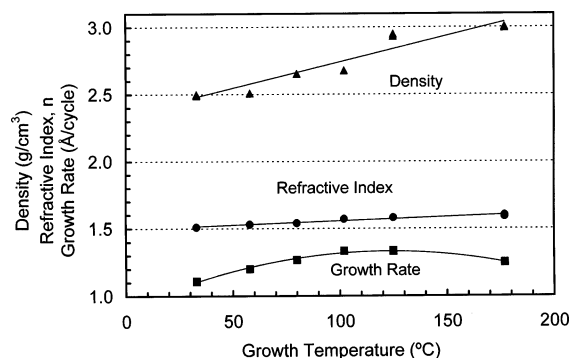


Figure 6. Ellipsometry data for Al_2O_3 ALD films grown using 300 reaction cycles on Si(100) substrates. The refractive index, growth rate, and density (calculated using ellipsometry and QCM data) are plotted versus growth temperatures from 33 to 177 °C.

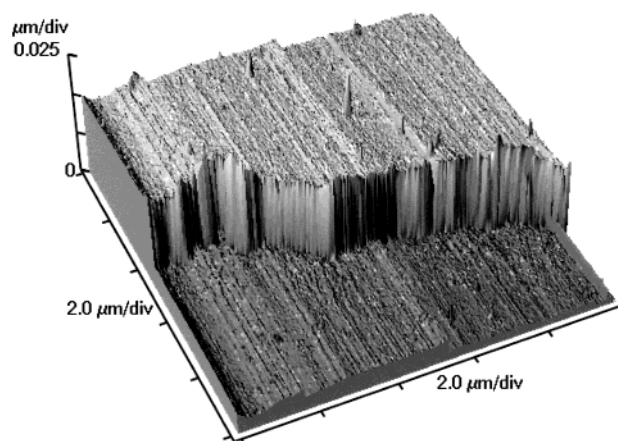


Figure 7. AFM image ($10 \times 10 \mu\text{m}^2$) used to determine the thickness of an Al_2O_3 ALD film grown at 58 °C using 300 ALD cycles on a Si(100) substrate. The step was created by masking part of the sample with aluminum tape during Al_2O_3 ALD. The average step height is 43 nm.

ALD. The average step height in this image is 43 nm. Film thicknesses determined by profilometry and AFM were within $\pm 10\%$ of the thicknesses derived by the ellipsometric measurements.

AFM was also used to determine the surface roughness of the Al_2O_3 ALD films. The low-temperature Al_2O_3 ALD films were all very smooth. The root-mean-squared (RMS) surface roughness for a $1 \times 1 \mu\text{m}^2$ area averaged 4 ± 1 Å. Growth temperature did not affect this surface roughness. The roughness of these films is also similar to that of Al_2O_3 ALD films grown at higher temperatures.^{9,18}

XRR scans for Al_2O_3 ALD films grown on Si(100) using 300 reaction cycles at temperatures from 33 to 177 °C are shown in Figure 8. The XRR scans were fitted to determine densities of the Al_2O_3 ALD films. These fits are also shown in Figure 8. The density of the Al_2O_3 ALD films derived by fitting the XRR measurements decreased from 3.06 g/cm³ at 177 °C to 2.46 g/cm³ at 33 °C. The XRR density results and comparison of all the density results are shown in Figure 9.

D. Electrical Characterization. Current–voltage (IV) and capacitance–voltage (CV) measurements were performed on the low-temperature Al_2O_3 ALD films. The

(18) Elam, J. W.; Sechrist, Z. A.; George, S. M. *Thin Solid Films* **2002**, *414*, 43.

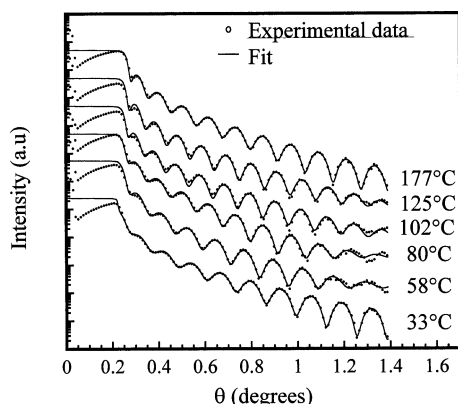


Figure 8. XRR scans for Al₂O₃ ALD films grown on Si(100) using 300 reaction cycles versus growth temperature from 33 to 177 °C. The fits to the XRR data used to determine densities are shown by the solid lines.

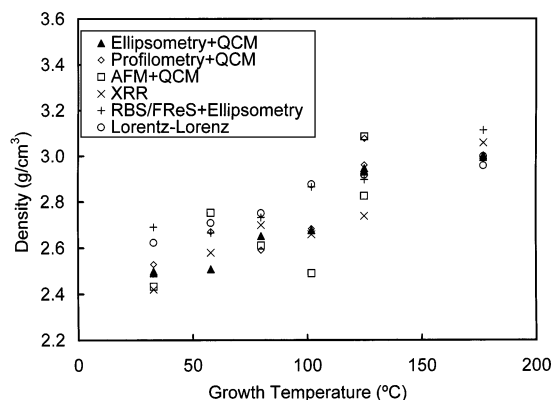


Figure 9. Density of Al₂O₃ ALD films versus growth temperature from 33 to 177 °C for the various methods.

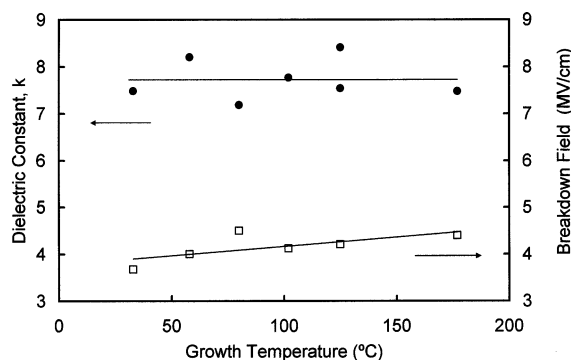


Figure 10. Electrical properties of low-temperature Al₂O₃ ALD films grown using 300 reaction cycles on *n*-Si(100).

IV curve characteristics remained relatively constant versus growth temperature. Low leakage current densities of $<10^{-7}$ nA/cm² at a 5 V bias were measured even for Al₂O₃ ALD films grown at 33 °C. Growth temperature did not appear to affect the leakage currents.

The catastrophic breakdown field decreased slightly with decreasing growth temperature as shown in Figure 10. The breakdown field was 4.4 MV/cm at 177 °C and decreased to 3.7 MV/cm at 33 °C. In addition, there was a decrease in the percentage of spots tested that exhibited good insulating behavior at lower growth temperatures. Capacitance measurements revealed no observable trend versus growth temperature. Figure 10 reveals that the dielectric constants of the Al₂O₃ ALD

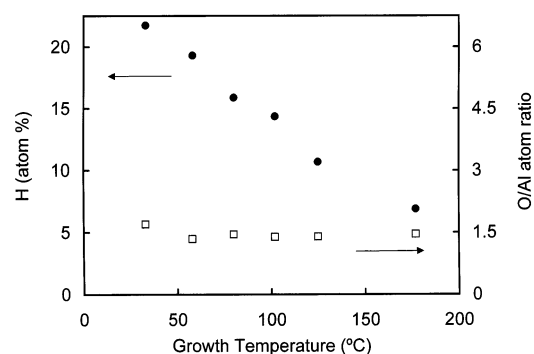


Figure 11. O/Al ratio and H concentrations for Al₂O₃ ALD films as determined by RBS and FReS versus growth temperatures from 33 to 177 °C.

films averaged $k = 7.7 \pm 0.4$ over the entire temperature range.

E. Elemental Analysis. Rutherford backscattering spectrometry (RBS) analysis measured O/Al ratios close to the expected 1.5 value as shown in Figure 11. The ratios ranged from 1.34 to 1.70. There was no systematic trend with growth temperature. Hydrogen concentrations measured by forward recoil spectrometry (FReS) increased with decreasing growth temperature as displayed in Figure 11. The H atom % in the Al₂O₃ ALD films increased from 6.9% at 177 °C to 21.7% at 33 °C. No other impurities were detected in the Al₂O₃ ALD films within the detection limit of the RBS.

F. Gas Diffusion. Gas diffusion tests with CO₂ were carried out on PET bottles coated with Al₂O₃ ALD films. Bottles were coated with 300 reaction cycles of Al₂O₃ ALD at 58 °C. This coating procedure should deposit a Al₂O₃ ALD film with a thickness of 360 Å. The CO₂ gas diffusion test revealed a CO₂ loss rate of 1.55% per week, or 2.91 cm³/(day bar cm²). This CO₂ loss rate for the Al₂O₃ ALD-coated bottle is a factor of ~ 1.6 lower than the CO₂ loss rate of an uncoated PET bottle. The ratio of these two CO₂ loss rates yields a barrier improvement factor (BIF) of ~ 1.6 .

Volumetric measurements of the PET bottles showed no change in volume as a result of Al₂O₃ ALD at 58 °C. PET bottles were also coated with 282 and 470 reaction cycles of Al₂O₃ ALD at a growth temperature of 80 °C and without the N₂ gas pressurization. These PET bottles deformed and increased in volume during deposition. The barrier improvements factors for these Al₂O₃ ALD-coated PET bottles were much smaller.

4. Discussion

A. Quartz Crystal Microbalance (QCM) Measurements. QCM studies showed that both the reactant exposure times and the nitrogen purge times required for Al₂O₃ ALD increased with decreasing temperatures. Longer reactant exposures at low temperatures are expected because the reaction is thermally activated.¹⁰ The purging of reactants, especially H₂O, takes longer at low temperatures because of slower desorption of H₂O from the reactor walls at lower temperatures.

The completion of the reactions took longer and became less defined, or "softer", at lower temperatures. This "soft" saturation is revealed by the small slope for the mass gain per cycle versus TMA and H₂O exposure at longer exposure times in Figure 4. These small slopes

indicate that either a complete reaction may not have been achieved or that the purge times may have become insufficient. Unfortunately, trying to achieve a complete reaction using reactant exposures of tens of seconds is inefficient in terms of time and reactant usage.

The maximum QCM mass gain per cycle of 39 ng/cm² was recorded at 125 °C as shown in Table 1. QCM measurements can be employed to calculate film thicknesses. These thickness calculations rely on known density values. For amorphous materials such as the Al₂O₃ ALD films grown at low temperatures, the density may change with growth temperature. Consequently, additional independent thickness measurements are required to derive the density from the QCM mass measurements.

B. Thickness Measurements and Al₂O₃ ALD Growth Rates. The agreement between the different methods of measuring Al₂O₃ ALD film thicknesses is quite good. Ellipsometric data exhibit less scatter than most of the other methods. The growth rate versus growth temperature obtained by ellipsometry displays a very smooth dependence in Figure 6. However, ellipsometry data depend on fitting several parameters to obtain a film thickness. This modeling can also be complicated by the presence of an interfacial SiO₂ layer.¹¹ Profilometry and AFM step height measurements are more direct determinations of film thickness but tend to be less precise. These measurements depend on the presence of a well-defined, sharp step edge that is not always easy to obtain. However, the film thicknesses obtained by profilometry and AFM agreed fairly well with the film thicknesses obtained by ellipsometry and XRR methods.

The Al₂O₃ ALD growth rates shown in Figure 6 reach a maximum of 1.33 Å/cycle at 100 and 125 °C. A previous study observed the maximum Al₂O₃ ALD growth rate of 1.1 Å/cycle at 177 °C.⁹ The position of this maximum was explained by the thermal activation required for the reaction at lower temperatures and decreasing Al–OH and Al–CH₃ surface coverages at higher temperatures.⁹ The growth rate is determined by reaction kinetics and necessary surface species.^{9,10} There are higher surface coverages at low temperatures, but slower reaction kinetics because of the thermal activation barrier. The reaction kinetics are more rapid at higher temperatures, but the growth rate is limited by the lower surface coverages.

C. Density. Figure 9 shows the densities of the Al₂O₃ ALD films as determined by a number of different methods. Densities were calculated on the basis of QCM, AFM, ellipsometry, profilometry, XRR, and RBS/FReS data. The density of the Al₂O₃ ALD films decreased with decreasing growth temperature based on all the different methods. Furthermore, the density values derived from the different methods agree fairly well with each other. Average densities ranged from 3.0 g/cm³ at 177 °C to 2.5 g/cm³ at 33 °C.

The densities of these low-temperature Al₂O₃ ALD films are significantly lower than the 3.5–3.7 g/cm³ value typically reported for amorphous Al₂O₃.^{19,20} The

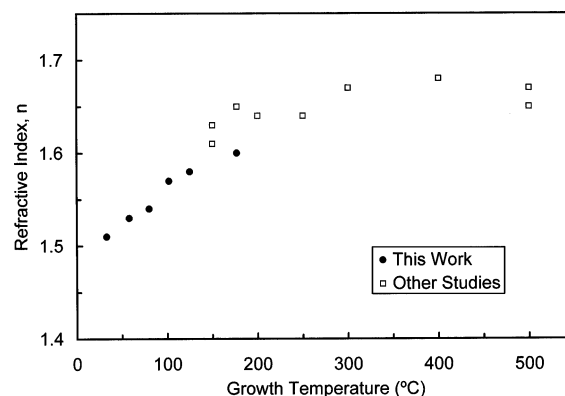


Figure 12. Refractive index, n , of the Al₂O₃ ALD films versus growth temperature from 33 to 177 °C and comparisons to results from other Al₂O₃ ALD studies at higher temperatures.^{9,12–15,21}

density of 3.0 g/cm³ at 177 °C is also lower than the density of 3.5 g/cm³ derived in a previous study of Al₂O₃ ALD films.⁹ That earlier study derived the density from the refractive index of the film and the Lorentz–Lorenz relationship assuming the optical constants of crystalline Al₂O₃. This assumption may not be correct because the Al₂O₃ ALD film is amorphous. The data in the current study are consistent with an average density of 3.0 g/cm³ at 177 °C based on many different types of measurements.

The density versus growth temperature has also been calculated using the Lorentz–Lorenz relationship.⁹ Starting with the density of 3.0 g/cm³ at 177 °C, densities for the Al₂O₃ ALD films grown at lower temperature were determined on the basis of their refractive indices, n . Figure 9 shows that the densities derived using the Lorentz–Lorenz relationship yield good agreement with the other Al₂O₃ ALD film densities.

D. Optical and Electrical Properties. Figure 6 shows that the refractive index of the Al₂O₃ ALD films decreased slightly with decreasing growth temperatures. This trend has been reported elsewhere and was attributed to decreased density and to increased impurity levels in films grown at lower temperatures.^{8,14} Figure 12 shows the refractive index of the low-temperature Al₂O₃ ALD films compared with the refractive index of Al₂O₃ ALD films measured in other studies.^{9,12–15,21} There is good agreement between the refractive indices in the region of overlap between 150 and 200 °C.

The refractive index increases with increasing growth temperature up to ~300 °C. The refractive index is then constant at $n \approx 1.67$ for growth temperatures between 300 and 500 °C. For comparison, the crystalline α -Al₂O₃ sapphire form of alumina has a refractive index of $n = 1.76$.¹⁵ This comparison indicates that the amorphous Al₂O₃ ALD film with $n \approx 1.67$ will densify further upon crystallization. This densification could lead to tensile stress and film cracking.

IV and CV measurements revealed good electrical properties for films grown at low temperatures. The decreasing breakdown field with decreasing growth temperature shown in Figure 10 may result from the decreasing density or the increased hydrogen concentra-

(19) Grey, D. E., Coord. Ed. *American Institute of Physics Handbook*; American Institute of Physics: New York, 1982.

(20) Weast, R. C., Ed. *CRC Handbook of Chemistry and Physics*; CRC Press: Boca Raton, FL, 1983–84.

(21) Kattelus, H.; Ylilammi, M.; Saarilahti, J.; Antson, J.; Lindfors, S. *Thin Solid Films* **1993**, 225, 296.

tion in the Al₂O₃ ALD films grown at lower temperatures. Figure 10 also shows that the dielectric constant did not decrease with decreasing growth temperatures. However, the scatter in the measurements may have masked a small change.

E. Film Composition. The RBS analysis of the Al₂O₃ ALD films obtained O/Al ratios close to the expected ratio of 1.5. In addition, FReS analysis revealed hydrogen concentrations in Figure 11 that increased with decreasing growth temperatures. The increasing hydrogen concentrations continue a trend that was observed in a previous study for Al₂O₃ ALD growth temperatures from 350 to 125 °C.¹¹ The increasing hydrogen concentration at low temperatures may be directly related to the lower density of the Al₂O₃ ALD films at lower growth temperature.

At lower temperatures, the hydroxyl surface coverage is higher on Al₂O₃ surfaces.^{9,10} In addition, the TMA reaction with the Al–OH surface species groups does not go to completion at low temperatures.^{9,10} During Al₂O₃ ALD, the hydroxyl species can build up in the growing Al₂O₃ film. At 180 °C, the hydroxyl concentration in the film after 10 AB cycles is equal to approximately the full hydroxyl coverage.¹⁰ Annealing at 1000 K can reduce hydroxyl accumulation in Al₂O₃ ALD films.¹⁰ These previous studies support the idea that the H atoms in the low-temperature Al₂O₃ ALD films are present in the form of Al–OH species.

Despite the high hydrogen concentrations at low temperatures, the Al₂O₃ ALD films still exhibited remarkably good properties. Low-temperature Al₂O₃ ALD films may be used for various applications where the high hydrogen concentration is not crucial. On the basis of the results at 33 °C, growing Al₂O₃ ALD films at room temperature is possible. The major problem is slow H₂O desorption from the reactor walls and very long required H₂O purge times. Shorter cycle times could be achieved using a modified reactor design and alternate oxygen sources such as N₂O,²² NO₂,¹⁶ or alkoxides.²³

F. Gas Diffusion Tests. The PET bottles coated with 300 reaction cycles of Al₂O₃ ALD at 58 °C displayed a decrease in CO₂ gas diffusion rates. However, lower CO₂ diffusion rates and higher barrier improvement factors

(BIF) are desired for commercial applications. Light microscopy images of the surface of the PET bottle revealed apparent scratches and/or cracks on the surface of the Al₂O₃ ALD-coated bottles. These scratches and/or cracks may explain the low BIF for these Al₂O₃ ALD films compared with typical BIFs for SiO₂ coatings.²⁴

5. Conclusions

Al₂O₃ ALD growth has been demonstrated at temperatures as low as 33 °C. Many of the properties of these low-temperature Al₂O₃ ALD films were comparable with the properties of Al₂O₃ ALD films grown at higher temperatures of ≥177 °C. The low-temperature Al₂O₃ ALD films exhibited very low surface roughness values, low leakage currents, high dielectric constants, and growth rates in excess of 1 Å/cycle. Good thin film properties were observed despite decreasing densities and increasing hydrogen concentrations observed at lower temperatures. Increased ALD cycle times were necessary at lower temperatures because of the slower reaction rates and longer required purge times for the H₂O reactant. Improvements in reactor design and the use of alternate oxygen sources could help overcome this problem. Low-temperature Al₂O₃ ALD may have applications for coating thermally fragile substrates such as organic, polymeric, or biological material. As a demonstration of the possible applications, low-temperature Al₂O₃ ALD films were grown on PET bottles to reduce gas diffusion. The Al₂O₃ ALD-coated PET bottles displayed lower CO₂ gas diffusion rates than uncoated PET bottles.

Acknowledgment. Funding for this research was research was provided by Applied Films Corporation. Additional support was provided by the Air Force Office of Scientific Research. We thank Russell Black and Elisabeth Sommer at Applied Films Corp. for providing the PET bottles and for performing CO₂ gas diffusion tests on the PET bottles coated with Al₂O₃ ALD films. Yongqiang Wang at the Ion Beam Analysis Laboratory in the Institute of Technology Characterization Facility at the University of Minnesota performed the RBS and FReS analysis of the Al₂O₃ ALD samples.

CM0304546

(22) Kumagai, H.; Toyoda, K.; Matsumoto, M.; Obara, M. *Jpn. J. Appl. Phys.* **1993**, *32*, 6137.

(23) Ritala, M.; Kukli, K.; Rahtu, A.; Raisanen, P. I.; Leskela, M.; Sajavaara, T.; Keinonen, J. *Science* **2000**, *288*, 319.

(24) Chatham, H. *Surf. Coat. Technol.* **1996**, *78*, 1.